

Effect of different casting methods on microstructure and mechanical properties of Mg-10Gd-3Y-0.6Zr alloy

DING Zhi-bing, LU Ruo-peng, HOU Hua, ZHAO Yu-hong

(School of Materials Science and Engineering, North University of China, Taiyuan 030051, China)

Abstract: The effects of two different casting methods on the microstructures and mechanical properties of as-cast and T6-cast states of Mg-10Gd-3Y-0.6Zr alloy were studied by using metal mold casting and squeeze casting. The results show that the microstructure of Mg-10Gd-3Y-0.6Zr alloy is mainly composed of α -Mg primary phase and $\text{Mg}_{24}(\text{Gd}, \text{Y})_5$ eutectic phase. The squeeze cast grains are small with a dendrite like morphology, and the tensile strength of the alloy in T6 state can reach 285 MPa. While the metal grains are coarse, the eutectic phases are distributed in the grain boundary, and the tensile strength of the alloy in T6 state is only 250 MPa.

Key words: squeeze casting; metal mold casting; Mg-10Gd-3Y-0.6Zr alloy; microstructure; mechanical property

CLD number: O614.22

Document code: A

Article ID: 1674-8042(2018)02-0194-05

doi: 10.3969/j.issn.1674-8042.2018.02.015

0 Introduction

Magnesium alloys are of great potential to be used in the aerospace, military, biomedical devices and automotive industries because of their low density, high specific strength, good damping performance and excellent machinability^[1-4]. However, low hardness, low strength, low modulus, low wear resistance and high thermal expansion coefficient of magnesium alloy restrict its wide applications.

Gd, Y and Zr are the important alloying elements of Mg-Gd-Y-Zr which greatly influence the alloy microstructures and mechanical properties^[5,6]. He et al.^[7] reports a four-stage precipitation process of Mg-10Gd-3Y-0.4Zr alloy aged at 250 °C, i. e., α -Mg supersaturated solid solution (S. S. S. S.) \rightarrow metastable β' (D019) \rightarrow metastable β' (cbco) \rightarrow metastable β_1 (fcc) \rightarrow stable β (fcc). It is reported that the metastable β' is responsible for the peak hardness and the most strengthening phase in Mg-Gd-Y-Zr alloy^[8].

At present, most research of Mg-Gd-Y-Zr alloy is based on the metal casting, while the research on squeeze casting is relatively less. As a modern

method of manufacturing technology near net forming, squeeze casting can promote the grain refinement and avoid casting porosity, shrinkage, porosity and other defects effectively, which has been widely used in automotive, military, marine and aviation fields^[9-13]. The microstructures and mechanical properties of two kinds of casting process of Mg-10Gd-3Y-0.6Zr alloy were studied systematically to provide technical basis for the applications of alloy.

1 Experimental procedure

To obtain Mg-10Gd-3Y-0.6Zr alloy, Mg-30%Gd, Mg-30%Y, Mg-30%Zr master alloys and pure Mg were melted in a medium frequency induction heating furnace by using a small mild steel crucible under a protective argon atmosphere at 780 °C. When the furnace was cooled to 730 °C, the metal mold and the squeeze casting mold were cast, respectively. Squeeze casting equipment is YB32-100B four column universal hydraulic machine.

In this test, the mold as shown in Fig. 1(a) is end of injection mold with serpentine pouring channel and

Received date: 2017-11-01

Foundation items: International Cooperation Project of the Ministry of Science and Technology of China (No. 2014DFA50320); National Natural Science Foundation of China (Nos. 51674226, 51574207, 51574206, 51204147, 51274175); International Science and Technology Cooperation Project of Shanxi Province (Nos. 2013081017, 2012081013)

Corresponding author: HOU Hua (houhua@263.net)

two large risers, which has very good effect on slag and can also make metal liquid filling smoothly to effectively ensure the quality of castings. Squeeze casting mold is simple, as shown in Fig. 1(b), and the shape of the casting is small box. According to the previous experimental experience^[14,15], the extrusion pressure of this experiment is set to

100 MPa, and the holding time is 20 s. Metal and squeeze casting molds are both preheated to 150 °C. The heat treatment of alloy samples is as follows: the solid solution treatment temperature is 500 °C for 8 h, followed by an immediate water quenching, then it is subsequently aged at 220 °C for 16 h in an air furnace.

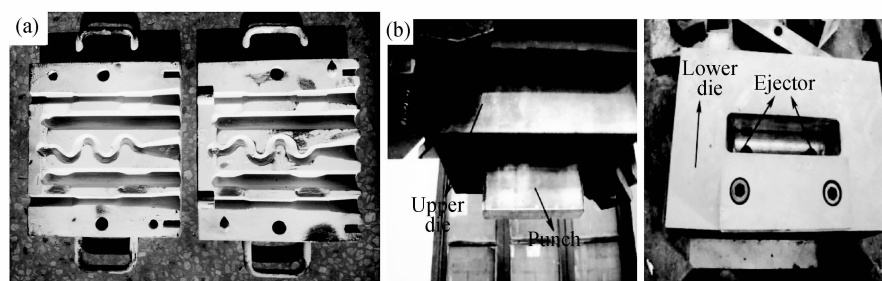


Fig. 1 Metal mold (a) and squeeze casting mold (b)

The samples for optical microscope (OM) and scanning electron microscope (SEM) analyses are prepared by the standard technique of grinding with SiC abrasive paper and polishing with MgO suspension solution, followed by etching in 4% (φ) nital solution. Phase analysis is conducted by using Rigaku D/MAX2500PC X-ray diffractometer with a copper target at scanning angles from 20° to 90° and scanning speed of 15 (°)/min. The average grain size (d) is measured by analyzing the optical micrographs with the mean linear intercept technique (ASTM E112-96). At least 300 grain boundaries are counted for each alloy.

Vickers hardness testing is taken by using load of 19.6 N for 15 s, where at least ten points are measured for each alloy. Tensile tests mentioned above are performed at a crosshead speed of 1.5 mm/min, according to the relevant standard of using cylindrical specimen (Fig. 2) with marked dimension of 25 mm gauge length and 5 mm diameter. All tensile tests are carried out on a Zwick/Roell Z020 tensile testing machine. An average of three measurements was used. The fracture surfaces were examined by SEM.

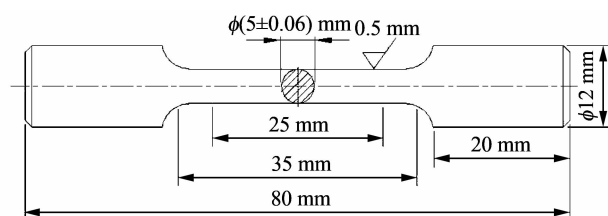


Fig. 2 Shape and size of tensile specimen

2 Results and discussion

2.1 Microstructures

Fig. 3 shows the optical micrographs of the as-cast samples obtained by the metal mold casting and the squeeze casting. The average grain sizes of metal mold and squeeze casting alloys are 43 μm and 37 μm , respectively. It can be seen that α -Mg grains are surrounded by a network-shaped eutectic phase in the Fig. 3(a). The squeeze cast grains are small, which are dendrite like morphology, and the secondary dendrite arms are connected to each other with a net shape.

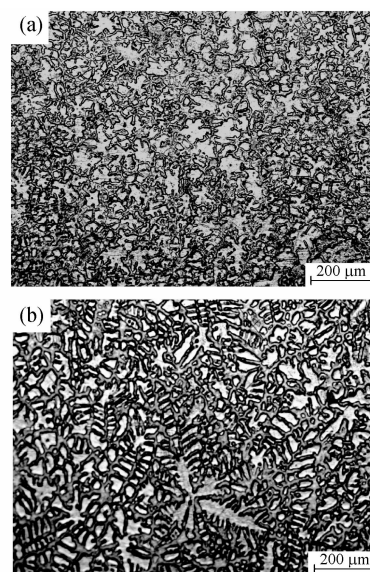


Fig. 3 Optical micrographs of as-cast alloy cast of metal mold (a) and squeeze cast (b)

Corresponding to the X-ray diffraction (XRD) curves given in Fig. 4, it can be identified that the as-cast alloys obtained by the two methods mainly consist of α -Mg and $\text{Mg}_{24}(\text{Gd}, \text{Y})_5$.

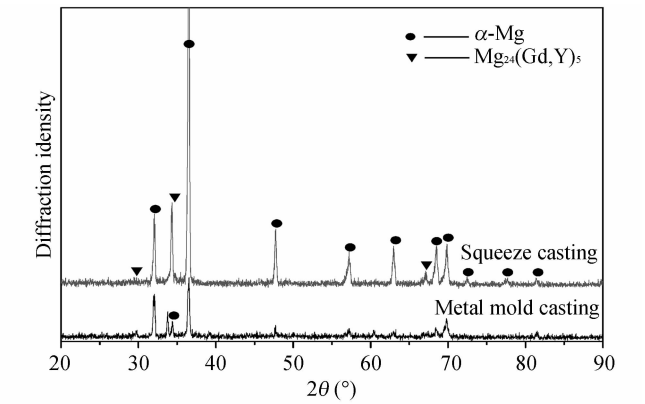


Fig. 4 XRD patterns of as-cast alloy in metal mold and squeeze cast

The microstructures of T6-cast alloy ($500\text{ }^{\circ}\text{C} \times 8\text{ h}$ solution treated $+220\text{ }^{\circ}\text{C} \times 16\text{ h}$ aging treatment) obtained by the methods of metal mold and squeeze casting are shown in Fig. 5.

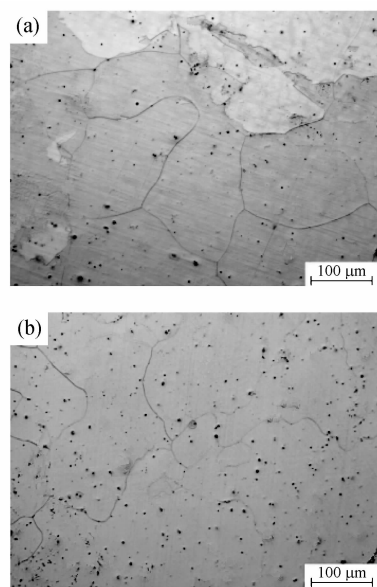


Fig. 5 Optical microstructures of T6-cast alloy by metal mold (a) and squeeze cast (b)

In Fig. (5), grain growth phenomenon is obvious, and the eutectic phase of $\text{Mg}_{24}(\text{Gd}, \text{Y})_5$ has disappeared, leaving only the clear boundary and being continuous together. It can be seen that a lot of black granular materials mainly distribute in the grain boundary, and scanning electron microscope analysis reveals that the black granular materials are massive phase and some spherical Zr core (shown in Fig. 5). It can be seen from Figs. 5(a) and (b) that

the phase distribution of the samples in the squeeze casting T6 state is more and more uniform, and the bulk phase of the metal casting sample is relatively small, and the dispersion is high. This is also the reason why the mechanical properties of extruded T6 samples are better than the metal casting.

Fig. 6 shows the SEM image of cuboid-shaped phase in the T6-cast alloy and the EDS element point results of cuboid-shaped phases. It can be seen that the cuboid-shaped phases mainly distribute at the grain boundaries, and their sizes are about $1\text{--}4\text{ }\mu\text{m}$. According to the EDS results, it can be identified that these cuboid-shaped phases are compound with high contents of the Gd and Y elements, which are about 56% (mass fraction) in total. According to the results in Ref. [7], the cuboid-shaped phases have face-centered cubic structure, and lattice constant is 5.6 nm.

Fig. 5 shows that the squeeze casting is more conducive to the precipitation of the block phase, which is also the reason why the squeeze casting is superior to the metal casting.

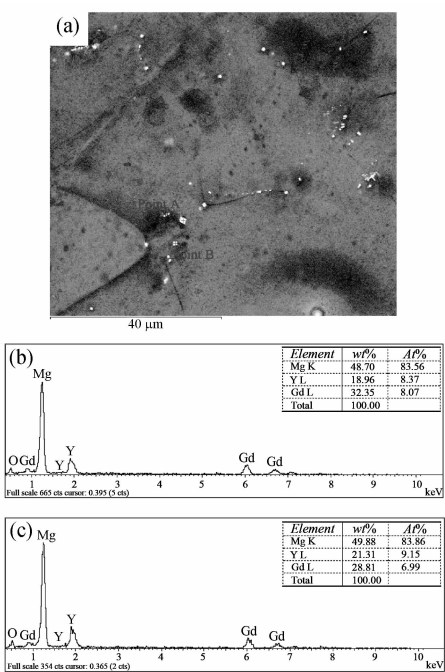


Fig. 6 SEM image of T6-cast alloy (a) and EDS results of cuboid-shaped phases point A (b) and point B (c)

2. 2 Mechanical properties

It can be seen from Fig. 7 that there is little difference in the mechanical properties of as-cast Mg-10Gd-3Y-0.6Zr alloy under metal mold and squeeze casting. The tensile strength of the squeeze casting samples is 183 MPa, so the tensile strength and

elongation are slightly higher than those of the metal mold casting samples. After solid solution, the strength of the squeeze casting samples is decreased, and the elongation is increased obviously, while the mechanical properties of the metal mold casting samples have not changed. After T6 treatment, the tensile strength is increased obviously, and the tensile strength of squeeze casting alloys reaches 285 MPa, which is higher than that of metal mold casting alloys about 35 MPa.

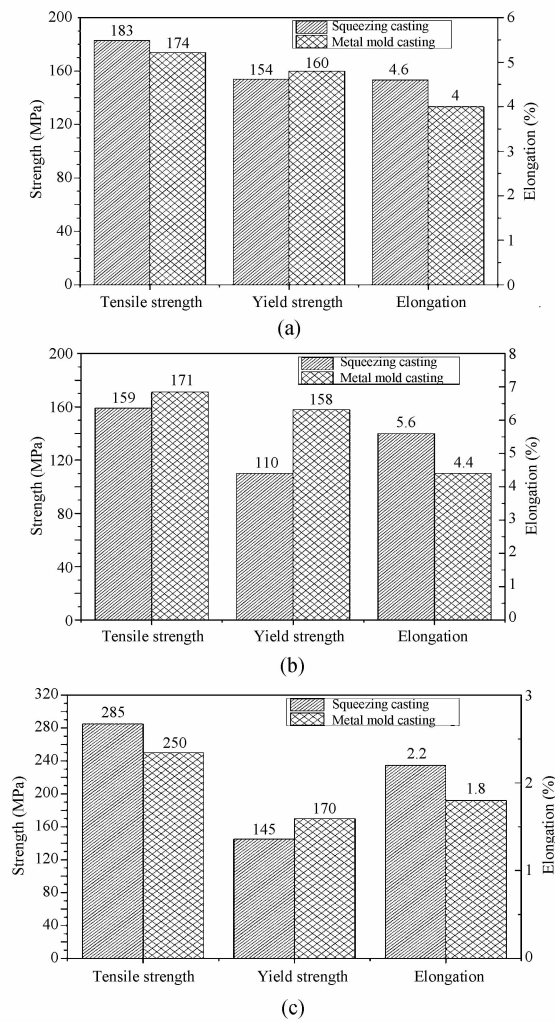


Fig. 7 Tensile mechanical properties of metal mold and squeeze cast specimens (a) as cast, (b) solid solution, (c) T6 state

2.3 Fractography

Fig.8 shows the fracture morphologies of the samples obtained by two methods of metal mold casting and squeeze casting. The fractures of as-cast alloy are rich in uneven distribution of small dimples and tear ridges, cleavage facets of small size and smooth distribution. After solid solution, the dimples become less, and cleavage planes become

wide. After T6 treatment, two samples of dimples become fewer, tearing edges become less, cleavage planes become more obvious, and the fracture is brittle fracture obviously.

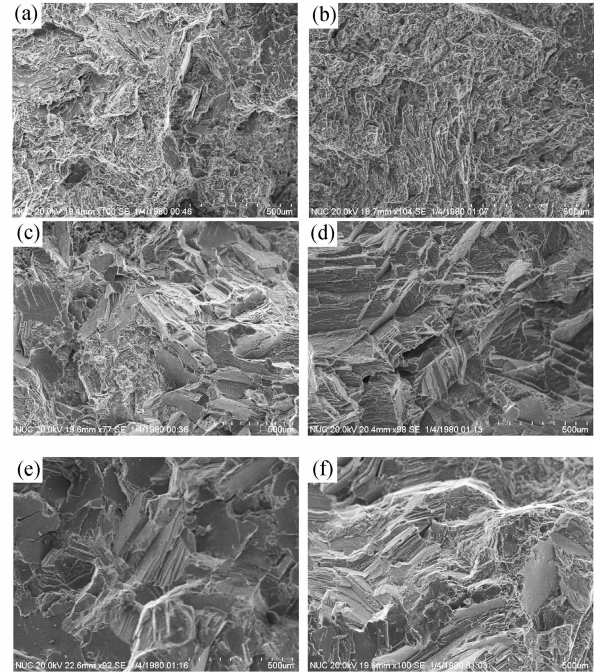


Fig. 8 Tensile fracture morphologies of metal (a, c, e) and squeeze (b, d, f) cast specimens, (a, b) as cast, (c, d) solid solution, (e, f) T6 state

3 Conclusions

1) The microstructure of Mg-10Gd-3Y-0.6Zr alloy is mainly composed of α -Mg primary phase and $\text{Mg}_{24}(\text{Gd}, \text{Y})_5$ eutectic phase. The squeeze cast grains are small, which are dendrite like morphology, and the secondary dendrite arm are connected to each other with a net shape, and the metal grains are coarse. After T6 treatment, the eutectic phase disappears; the grain grows up obviously; the grain boundary is clear and fine, and the block phases precipitate in the grain.

2) In terms of the mechanical properties, the squeeze casting is better than the metal casting, and the tensile strength of the squeeze casting under the T6 state is 285 MPa.

3) The tensile fracture mode of squeeze casting samples is changed from combination of transgranular plus dimple-like fracture of as-cast to intergranular fracture of T6-cast.

References

- [1] Liu S P, Jie X P, Y H, et al. Influence of SiC particles size on structure and properties of az61 Mg-based compos-

- ites. Hot Working Technology, 2009, 38(18): 61-67.
- [2] Wang X Q, Li Q A, Zhang X Y. Effects of yttrium and neodymium on microstructure and mechanical properties of AZ81 magnesium alloy. Rare Metal Materials and Engineering, 2008, 37(1): 62-65.
- [3] Fu P H, Wang Q D, Jiang H Y, et al. Development of research on magnesium alloy melting technology. Foundry Technology, 2005, 26(6): 489-492.
- [4] Xu C, Zheng M Y, Xu S W, et al. Ultra high-strength Mg-Gd-Y-Zn-Zr alloy sheets processed by large-strain hot rolling and ageing. Materials Science and Engineering A, 2012, 547: 93-98.
- [5] Sun M, Wu G H, Wang W, et al. Effect of Zr on the microstructure, mechanical properties and corrosion resistance of Mg-10Gd-3Y magnesium alloy. Materials Science and Engineering A, 2009, 523(1-2): 145-151.
- [6] Chang J W, Guo X W, He S M, et al. Investigation of the corrosion for Mg-xGd-3Y-0.4Zr ($x=6, 8, 10, 12$ wt%) alloys in a peak-aged condition. Corrosion Science, 2008, 50(1): 166-177.
- [7] He S M, Zeng X Q, Peng L M, et al. Precipitation in a Mg-10Gd-3Y-0.4Zr (wt. %) alloy during isothermal ageing at 250 °C. Journal of Alloys and Compounds, 2006, 421(421): 309-313.
- [8] Jafari Nodooshan H R, Liu W C, Wu G H, et al. Effect of Gd content on microstructure and mechanical properties of Mg-Gd-Y-Zr alloys under peak-aged condition. Materials Science and Engineering A, 2014, 615: 79-86.
- [9] Zhou Y J, Liu J X. Research progress on particle reinforced magnesium matrix composite. Light Alloy Fabrication Technology, 2012, (2): 12-15.
- [10] Song L, Shao M. The Investigation of movement parameters in squeezing casting based on wavelet. China Foundry, 2014, 63: 26-29.
- [11] Zhang F Y, Yan H, Chen G X, et al. Optimization of preparing technology for SiCp/AZ61 magnesium matrix composites. Special Casting and Nonferrous Alloys, 2007, 27: 741-743.
- [12] Wu R R, Yuan Z, Li Q S, et al. Microstructure and properties of Al_2O_3 /Al aluminum matrix composites fabricated by squeeze process. Foundry, 2017, 66: 29-32.
- [13] Luo J X, Fan W Z, Chen X W, et al. Comprehensive control method of quality of squeeze casting parts. Special Casting and Nonferrous Alloys, 2016, 36(3): 256-260.
- [14] Du W B, Yan Z J, Wu Y F, et al. Conventional and novel fabrication of magnesium matrix composites. Rare Metal Materials and Engineering, 2009, 38: 560-564.
- [15] Wu J K, Wang Y M, Hou H, et al. Study on technologies of squeeze casting of SiCp/AZ91D magnesium composites. China Foundry, 2014, 63(4): 336-340.

不同铸造方法对 Mg-10Gd-3Y-0.6Zr 合金 组织形貌及力学性能的影响

丁志兵, 鲁若鹏, 侯华, 赵宇宏

(中北大学 材料科学与工程学院, 山西 太原 030051)

摘 要: 采用金属型和挤压铸造两种不同铸造方法对铸态和 T6 态 Mg-10Gd-3Y-0.6Zr 合金的组织形貌和力学性能进行研究。结果表明, Mg-10Gd-3Y-0.6Zr 合金铸态组织主要由 α -Mg 初生相和 $Mg_{24}(Gd, Y)_5$ 共晶相组成; 挤压铸造所得合金晶粒细小, 且呈枝晶状形貌, T6 态时合金抗拉强度可达 285 MPa; 金属型所得合金晶粒较粗大, 共晶相呈网状分布在晶界处, T6 态时合金抗拉强度只有 250 MPa。

关键词: 挤压铸造; 金属型铸造; Mg-10Gd-3Y-0.6Zr 合金; 组织形貌; 力学性能

引用格式: DING Zhi-bing, LU Ruo-peng, HOU Hua, et al. Effect of different casting methods on microstructure and mechanical properties of Mg-10Gd-3Y-0.6Zr alloy. Journal of Measurement Science and Instrumentation, 2018, 9(2): 194-198. [doi: 10.3969/j.issn.1674-8042.2018.02.015]